



HAL
open science

Pseudo-3D modelling of a surface-bonded Lamb wave source

Emmanuel Moulin, Sébastien Grondel, Mustapha Baouahi, Jamal Assaad

► **To cite this version:**

Emmanuel Moulin, Sébastien Grondel, Mustapha Baouahi, Jamal Assaad. Pseudo-3D modelling of a surface-bonded Lamb wave source. *Journal of the Acoustical Society of America*, 2006, 119, pp.2575-2578. 10.1121/1.2189447 . hal-00138727

HAL Id: hal-00138727

<https://hal.science/hal-00138727>

Submitted on 23 Oct 2023

HAL is a multi-disciplinary open access archive for the deposit and dissemination of scientific research documents, whether they are published or not. The documents may come from teaching and research institutions in France or abroad, or from public or private research centers.

L'archive ouverte pluridisciplinaire **HAL**, est destinée au dépôt et à la diffusion de documents scientifiques de niveau recherche, publiés ou non, émanant des établissements d'enseignement et de recherche français ou étrangers, des laboratoires publics ou privés.

Pseudo-3D modeling of a surface-bonded Lamb wave source (L)

Emmanuel Moulin,^{a)} Sébastien Grondel, Mustapha Baouahi, and Jamal Assaad
*IEMN, UMR CNRS 8520, OAE Department, Université de Valenciennes et du Hainaut Cambrésis,
Le Mont Houy, 59313 Valenciennes Cedex 9, France*

In this paper, a simple technique allowing the prediction of the Lamb wave field excited in an isotropic plate by a transducer of finite dimensions is presented. The basic idea is to separate the problem into two uncoupled parts. First, the Lamb wave excitation problem, in the plane defined by the thickness and width directions of the transducer, is treated. Then the source diffraction effects in the plane of the plate can be quantitatively estimated. The subsequent formulation thus offers a simple way of developing three-dimensional (3D) solutions from a two-dimensional (2D) modeling. Compared to a heavy full-3D numerical modeling, this technique appears to be a very satisfying alternative.

I. INTRODUCTION

For several years, Lamb wave testing has been seen as a promising technique for health monitoring of civil or aerospace structures. In order to make such monitoring faster, less expensive, and effortless, the integration of piezoelectric patches to the material has been considered.^{1,2} The behavior of such an integrated transducer and the type of waves emitted depend strongly on the nature of the host material and the insertion conditions. Then a proper modeling tool, allowing to take into account the whole complexity of the problem, is required.

In this context, previous works have focused on the development of a 2D hybrid technique for the modeling of plates containing integrated sources.³⁻⁵ The imposed plane-strain condition implied the infiniteness along one dimension, which is only a rough approximation of a bar-shaped transducer. In order to account for the finite length of an actual transducer, a 3D modeling is required. However, instead of developing unpractical full 3D numerical models, the idea suggested here is to uncouple the divergence effects in the plane of the plate from the mode characteristics with respect to the plate thickness.

This concept has already been presented in a previous paper⁶ and applied to multi-element sources for Lamb wave beam-steering.⁷ However, the simplistic approach used then only provided qualitative results. This paper aims at extending these works so that quantitative results are accessible, allowing direct comparison to experimental or 3D numerical results.

Up to now, only a very small number of works have dealt with 3D modeling of Lamb wave excitation by finite sources. Among them, a recent paper by Rose *et al.*⁸ is particularly noticeable. Based on Mindlin plate theory, the authors derived analytical solutions for point forces and bending moments and then deduced solutions for circular-or rectangular-shaped surface-mounted sources by spatial integration. However, the formulation is relatively delicate to handle and since Mindlin theory is an approximate plate model, a number of physical aspects are not correctly described (symmetric modes, higher order antisymmetric modes,...).

The modeling method proposed here is based on line- and point-source solutions derived from the works by Viktorov and Ditri, respectively.^{9,10} A remarkable synthesis and useful applications of these works have been presented by Wilcox.¹¹ Though not fundamentally different in nature, the formulation introduced in the present paper is more suited to the objective. As will be seen indeed, the link established with the normal mode expansion method¹² results in a very versatile and lightweight pseudo-3D modeling technique.

II. MODELING PRINCIPLE

A. Finite length excitation

Let us consider an isotropic plate with thickness d , excited by a given harmonic stress applied to a localized area of its upper surface (Fig. 1). The excitation area S is supposed to be rectangular shaped, with length L and width W . The applied stress profile is described by a function $\sigma_0(x, y)$ defined over S and representing the action of a transducer. In order to simplify the notations, all the derivations presented

^{a)}Electronic mail: emmanuel.moulin@univ-valenciennes.fr

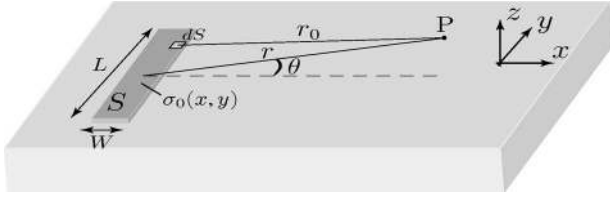


FIG. 1. Description of the problem geometry.

below will consider the normal component of the displacement on the plate surface only. If required, expressions for the transverse displacement or the displacement inside the plate thickness could be derived exactly the same way.

Assuming that a single Lamb wave is generated in the plate (this assumption can be released afterwards), the normal displacement du excited at a given point P of the plate upper surface by a small part dS with coordinates (x, y) of the actuation area can be deduced from the axisymmetric solution proposed by Ditri *et al.*¹⁰ This can be written in a compact form as

$$du = \frac{j\sigma_0(x, y)\Gamma k}{4\mu\Delta'} H_0^{(1)}(kr_0) e^{-j\omega t} dS, \quad (1)$$

where r_0 is the distance from the excitation point, k is the wave number of the considered Lamb wave, and Γ and Δ are functions depending on k and the material properties. They are representative of eigenmode-related features. Their complete expressions can be found in the literature¹⁰ whenever needed and thus will not be reminded here. The prime ' denotes derivation with respect to k . $H_0^{(1)}$ represents the zeroth-order Hankel function of the first kind. For conciseness, the term $e^{-j\omega t}$ will be omitted in the next equations.

Let us now consider the case of an excitation represented by separable variable functions:

$$\sigma_0(x, y) = \sigma_{0x}(x)\sigma_{0y}(y). \quad (2)$$

Here σ_{0x} will be supposed to depend on W only and σ_{0y} on L only. In the case of an actual transducer, such an assumption is acceptable provided L and W are different enough to allow the length and width vibration modes to be uncoupled.⁶

Considering a location far enough from the source so that $r \gg L, W$ yields

$$r_0 \approx r - x \cos \theta - y \sin \theta. \quad (3)$$

Then, by integrating Eq. (1) over the excitation area S and using the far-field asymptotical approximation of the Hankel function along with Eq. (3), the total normal displacement at a point P with polar coordinates (r, θ) can be expressed as

$$u(r, \theta) = \frac{j(1-j)\Gamma}{4\mu\sqrt{\pi}\Delta'} \sqrt{\frac{k}{r}} e^{jkr} \int_{-L/2}^{L/2} \sigma_{0y}(y) e^{-jky \sin \theta} dy \times \int_{-W/2}^{W/2} \sigma_{0x}(x) e^{-jkx \cos \theta} dx. \quad (4)$$

B. Infinite length excitation

Let us now consider the same plate, subject to an excitation defined by the same width W and the same applied stress function σ_{0x} as in the previous section. This case, however, will significantly differ from the previous one in that the length L will be considered infinite. In that case, a two-dimensional, plane-strain formulation is valid. Then the displacement at a given point, located at a distance r from the source, can be obtained by integration of a line-source solution. Such a solution can be derived from the work by Viktorov on wedge transducer excitation,⁹ which had also been applied by Wilcox.¹¹ This yields an expression of the form

$$u_{2D}(r) = \frac{j\Gamma}{2\mu\Delta'} e^{jkr} \int_{-W/2}^{W/2} \sigma_{0x}(x) e^{-jkx} dx, \quad (5)$$

where Γ and Δ are the same as in Eqs. (1) and (4).

By introducing the modal amplitude A_m for the given Lamb mode, derived from the 2D normal mode formalism,^{3,12} this displacement can also be written as

$$u_{2D}(r) = A_m u_m e^{jkr}, \quad (6)$$

where u_m is the modal displacement field (eigen vector) for the considered mode.

C. Connection of the 2D and 3D problems

Equations (4) and (5) are independently established from two geometrically different excitation cases. However, since the propagation medium (the solid plate) is supposed to be the same in both cases, it is no surprise that some eigenmode terms remain identical in both equations. This is indeed the case with Γ and Δ , as written above. Besides, the integrals over x are the same in Eqs. (4) and (5) if either the source width W is small compared to the wavelength or θ is small, or a combination of both.

In those conditions, comparison of these two equations and substitution of the above-mentioned identical terms yield the following relation between the finite-length and the 2D infinite-length solutions:

$$u(r, \theta) = \frac{(1-j)}{2\sqrt{\pi}} \sqrt{\frac{k}{r}} u_{2D}(r) \int_{-L/2}^{L/2} \sigma_{0y}(y) e^{-jky \sin \theta} dy \quad (7)$$

Then, by invoking Eq. (6), the finite-length displacement can finally be expressed as

$$u(r, \theta) = \frac{(1-j)}{2\sqrt{\pi}} \sqrt{\frac{k}{r}} A_m u_m e^{jkr} \int_{-L/2}^{L/2} \sigma_{0y}(y) e^{-jky \sin \theta} dy \quad (8)$$

In the case of an actual rectangular shaped surface-mounted transducer, it has been shown in a previous work⁶ that the excitation $\sigma_{0y}(y)$ could be considered uniform over the transducer length L , provided the condition $W/L \leq 0.4$ is ensured. In that case, Eq. (8) can be simplified as

$$u(r, \theta) = \frac{(1-j)}{\sqrt{\pi}} \sqrt{\frac{k}{r}} A_m u_m \frac{\sin(k(L/2)\sin \theta)}{k \sin \theta} e^{jkr}. \quad (9)$$

This equation is similar to the general formulation given in Ref. 6. In this previous work, however, the directivity

relation was obtained by merely using a basic scalar diffraction model, which constituted quite a rough approximation. This resulted in rather satisfying qualitative directivity predictions but an undetermined, frequency- and mode-dependent amplitude term remained. This made direct comparison to 3D numerical modeling or experimental results impossible. On the contrary, Eq. (9) of the present paper allows the displacement waveforms to be correctly predicted, even in the multi-mode case.

The first step of the pseudo-3D modeling scheme is the treatment of the 2D plane-strain problem (assuming L infinite). This provides the modal amplitudes A_m for the considered transducer width W . It should be noted that the actual transducer thickness and piezoelectric characteristics can also be taken into account if required. A complete description of the procedure can be found in previous works.³⁻⁵ Therefore, it will not be repeated here. Then, the third dimension is introduced by using Eq. (9). Hence, wave radiation in the (x, y) plane can be quantitatively characterized for each propagating mode. Finally, if required, summation of all mode contributions can be performed in order to obtain the total 3D displacement field in the plate.

III. APPLICATION TO A KNOWN EXCITATION

A. Problem description

In order to verify its pertinence and predicting ability, the modeling procedure will be applied to a simple case. We will consider a 3-mm-thick aluminum plate subject to a uniform pressure p_0 over the excitation area S as described in Fig. 1.

In such a simple situation, solution to the related 2D problem can be processed analytically. Details of the derivation can be found in Refs. 3 and 5. This yields

$$A_m = \frac{j\omega p_0 u_{mz}^*}{2kP_{mm}} \sin\left(\frac{kW}{2}\right) \quad (10)$$

with

$$P_{mm} = \frac{\omega}{2} \text{Im} \left[\int_{-d/2}^{d/2} (u_{mx}^* \sigma_{mxx} + u_{mz}^* \sigma_{mzx}) dz \right], \quad (11)$$

where Im and $*$ denote the imaginary part and the complex conjugate, respectively. u_m and σ_m are the modal displacement and stress tensors for the considered Lamb mode.

Though Eq. (9) has a meaning in a harmonic case only, transient excitations can be very classically dealt with using Fourier inversion.^{5,13}

B. Results and comments

The first example corresponds to a two-cycle rectangular-windowed sinusoid at 150 kHz. At this frequency-thickness product and considering an out-of-plane excitation, the first antisymmetric mode A_0 is practically the only excited mode. The excitation area is defined by $W=8$ mm and $L=20$ mm. The resulting normal displacement at a distance $r=45$ mm is presented in Fig. 2(a). The dashed line represents the 2D solution, derived from the normal

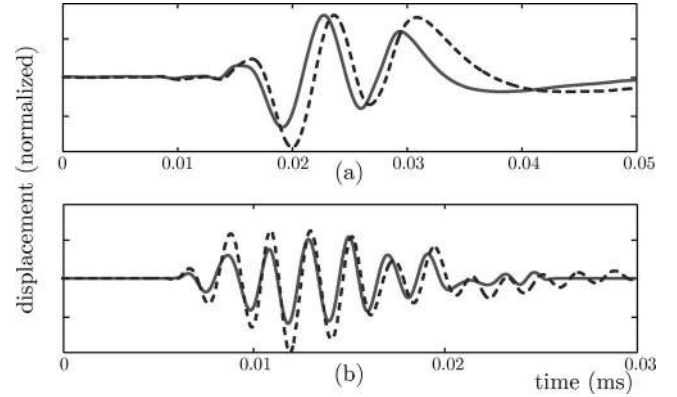


FIG. 2. Influence of 3D effects on the waveform shape (2D solution in dashed line, 3D solution in solid line). (a) Transducer size 8×20 mm, central frequency 150 kHz, $r=45$ mm, $\theta=0^\circ$. (b) Transducer size 6×20 mm, central frequency 475 kHz, $r=28$ mm, $\theta=0^\circ$.

mode formalism. Application of Eq. (9), corresponding to the pseudo-3D solution, is represented by the solid line.

A second demonstrative example is presented in Fig. 2(b). It corresponds to a multi-modal case. The excitation is a five-cycle sine-windowed sinusoid at 475 kHz and the source dimensions are $W=6$ mm and $L=20$ mm. The considered propagation distance is $r=28$ mm. All three modes: A_0 , S_0 and A_1 are excited, though with different modal amplitudes. Here again, the solid and dashed lines represent the 3D and 2D results, respectively.

As shown here, taking into account the 3D behavior can lead to significant changes in the received waveforms. This can be easily interpreted from the form of Eq. (9). In addition to a mere amplitude decay proportional to $1/\sqrt{r}$ and related to the beam divergence in the (x, y) plane, the \sqrt{k} factor disturbs the dispersive effects in the wave propagation. Indeed, components with low frequencies tend to be attenuated whereas higher frequency components tend to be amplified. Therefore the frequential reconstruction of the signal naturally yields modified waveforms. Besides, since S_0 and A_1 have smaller wave numbers than A_0 , they appear more attenuated in the 3D case than in the 2D one. This results logically in a visible modification of the global waveform.

C. Comparison to numerical predictions

For quantitative validation purpose, both examples will be compared to results from a 3D finite element modeling (FEM). The excitation is modeled by applying normal point forces to the surface nodes in the corresponding area. The finite element mesh definition is guided by two, rather contradictory, criteria. First, the lateral dimensions of the plate have to be large enough so that no reflection pollutes the incident wave packets. Then, the elements should be numerous enough so that their sizes are smaller than a quarter of the shorter wavelength.¹⁴ This ordinarily results in a rather cumbersome 3D mesh and, subsequently, in a huge memory and time consumption. Therefore, only a limited number of test cases can be reasonably treated in this way.

The obtained results are shown in Figs. 3(a) and 3(b).

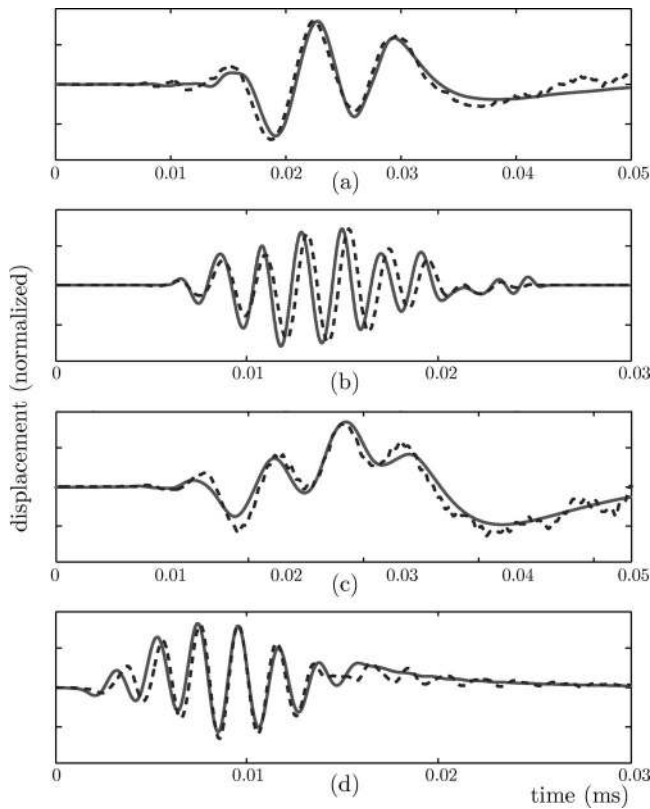


FIG. 3. Comparison of pseudo-3D solutions (solid) to 3D-FEM results (dashed). (a) Transducer size 8×20 mm, central frequency 150 kHz, $r = 45$ mm, $\theta = 0^\circ$. (b) Transducer size 6×20 mm, central frequency 475 kHz, $r = 28$ mm, $\theta = 0^\circ$. (c) Transducer size 8×20 mm, central frequency 150 kHz, $r = 45$ mm, $\theta = 50^\circ$. (d) Transducer size 6×20 mm, central frequency 475 kHz, $r = 12$ mm, $\theta = 35^\circ$.

The dashed lines correspond to the FEM results whereas the solid lines represent the same pseudo-3D results as in the previous section.

As can be seen, there is a very good agreement between the two sets of curves. Both the waveform shapes as well as the relative mode amplitudes are correctly predicted. Additionally, in order to provide validation for off-axis predictions, some results for $\theta \neq 0$ are presented in Figs. 3(c) and 3(d). These results correspond to the same excitation cases as in Figs. 3(a) and 3(b), respectively. The first curve [Fig. 3(c)] is obtained at $r = 45$ mm, $\theta = 50^\circ$. The second one [Fig. 3(d)] corresponds to $r = 12$ mm, $\theta = 35^\circ$. These comparisons clearly demonstrate the ability of the hybrid pseudo-3D technique to provide quantitative results with a satisfying accuracy.

IV. CONCLUSION

This work was concerned with the problem of plate wave generation by a surface-mounted transducer with finite dimensions. In many practical cases, the 3D source effects

cannot be neglected without leading to significantly erroneous results. As it has been verified indeed, both the waveform shapes and the mode amplitudes can be strongly affected by the finite length of the emitter.

Relying on existing works, it has been shown how the 3D characterization could be achieved by merely applying a corrective term to a 2D result. The formulation introduced allows the use of the normal mode expansion technique for solving the 2D problem, which results in a very convenient, polyvalent, and easy-to-use model. Comparison with results provided by a full-3D finite element computation have demonstrated the quantitative validity of the technique.

Besides, in previous works, a 2D hybrid FEM-normal mode technique has been successfully applied and has already been subject to adaptations to physical effects of growing complexity (anisotropy, attenuation,...). Then, the introduction of such effects into the pseudo-3D modeling could be considered without starting from the basis again.

- ¹R. S. C. Monkhouse, P. D. Wilcox, and P. Cawley, "Flexible interdigital pdfd lamb wave transducers for the development of smart structures," *Rev. Prog. Quant. Nondestr. Eval.* **16**, 877–884 (1997).
- ²J.-B. Ihn and F.-K. Chang, "Detection and monitoring of hidden fatigue crack growth using a built-in piezoelectric sensor/actuator network: I. diagnostics," *Smart Mater. Struct.* **13**, 609–620 (2004).
- ³E. Moulin, J. Assaad, C. Delebarre, and D. Osmont, "Modeling of lamb waves generated by integrated transducers in composite plates using a coupled finite element-normal modes expansion method," *J. Acoust. Soc. Am.* **107**, 87–94 (2000).
- ⁴S. Grondel, C. Paget, C. Delebarre, J. Assaad, and K. Levin, "Design of optimal configuration for generating a_0 lamb mode in a composite plate using piezoceramic transducers," *J. Acoust. Soc. Am.* **112**, 84–90 (2002).
- ⁵L. Duquenne, E. Moulin, J. Assaad, and S. Grondel, "Transient modeling of lamb waves generated in viscoelastic materials by surface bonded piezoelectric transducers," *J. Acoust. Soc. Am.* **116**, 133–141 (2004).
- ⁶E. Moulin, N. Bourasseau, J. Assaad, and C. Delebarre, "Directivity of integrated piezoelectric lamb wave sources," in *Proc. IEEE Ultrason. Symp.* (IEEE, Atlanta, USA, 2001), pp. 1081–1084.
- ⁷E. Moulin, N. Bourasseau, J. Assaad, and C. Delebarre, in "Lamb wave beam-steering for integrated health monitoring applications," in *Proc. SPIE* (SPIE, San Diego, USA, 2003), pp. 124–131.
- ⁸L. R. F. Rose and C. H. Wang, "Mindlin plate theory for damage detection: Source solutions," *J. Acoust. Soc. Am.* **116**, 154–171 (2004).
- ⁹I. A. Viktorov, *Rayleigh and Lamb Waves* (Plenum, New York, 1967).
- ¹⁰J. J. Ditre, A. Pilarski, B. Pavlakovic, and J. L. Rose, "Generation of guided waves in a plate by axisymmetric normal surface loading," *Rev. Prog. Quant. Nondestr. Eval.* **13**, 133–140 (1994).
- ¹¹P. D. Wilcox, "Lamb wave inspection of large structures using permanently attached transducers," Ph.D. thesis, Imperial College, London, UK, 1998.
- ¹²B. A. Auld, *Acoustic Fields and Waves in Solids*, 2nd ed. (Krieger, Malabar, FL, 1990).
- ¹³L. Duquenne, E. Moulin, J. Assaad, and C. Delebarre, "Transient modeling of lamb wave generation by surface bonded piezoelectric transducers," in *Proc. SPIE Vol. 4763* (SPIE, Presqu'île de Giens, France, 2002), pp. 187–193.
- ¹⁴O. C. Zienkiewicz and R. L. Taylor, *The Finite Element Method*, 5th ed. (Butterworth-Heinemann, Oxford, MA, 2000).